*Published in: Applied Superconductivity (1996), vol. 4, iss. 10-11, pp. 507-517.*
*Status : Postprint (Author's version)*

# GROWTH FEATURES AND INTERGRANULAR CONNECTIVITY OF MELT PROCESSED YBCO

Wai Lo, Charles D. Dewhurst, David A. Cardwell,

Philippe Vanderbemden, Richard A. Doyle and Doug M. Astill

*IRC in Superconductivity, University of Cambridge, Madingley Road, Cambridge, CB3 OHE, U.K.*

**Abstract**

Large grain melt processed Y-Ba-Cu-O (YBCO) samples have been prepared by seeded and unseeded growth techniques. The current carrying ability within individual grains and across grain boundaries has been investigated and correlated with features in the microstructure of samples fabricated by both techniques. The development of an inhomogeneous, cell-like growth microstructure in seeded samples at distances ≈4 mm from the seed is related to a saturation in inclusion density and volume proportion of $Y_2BaCuO_5$ (Y211) particles. A significant decrease in critical current density is associated with this change over a wide temperature range. The resistance of high angle c-axis grain boundaries is observed to depend critically on the magnitude of the injection current whereas the intragranular resistance is not influenced significantly by this variable. $J_c$ of a grain boundary fabricated by unseeded melt growth is estimated to be less than 100 A $cm^{-2}$ at 77 K in zero applied field, which is more than two orders of magnitude lower than the intragranular $J_c$. Field screening measurements suggest that low angle grain boundaries do not form weak links between grains in modest magnetic fields and hence do not present a significant barrier to current flow.

## 1. INTRODUCTION

Textured (RE)-Ba-Cu-O [(RE)BCO] high temperature superconductors (HTS) have the potential to support transport currents in the presence of relatively large magnetic fields ( > 5 T) at liquid nitrogen temperatures and hence are candidate materials for practical conductor applications. A fundamental requirement of HTS materials for such applications, however, is that they exhibit a uniform, high critical current density ($J_c$) over long sample lengths or that they can be fabricated uniformly in short lengths and then joined by a suitable process to yield a high current carrying boundary.

Large, high $J_c$ superconducting pseudo-crystals of Y-Ba-Cu-O (YBCO), consisting of a superconducting $YB_2Cu_3O_{7-\delta}$ (Y123) crystal matrix containing non-superconducting $Y_2BaCuO_5$ (Y211) inclusions can be fabricated up to 7 cm in diameter [1] by a variety of melt processing and seeding techniques [2-9]. It has been well established that the superconducting transport properties of these materials, and $J_c$ in particular, depending critically on the presence and density of point defects (e.g. cation dopants and oxygen vacancies), line defects (e.g. dislocation), plane defects (e.g. twins), non-superconducting second-phase inclusion (e.g. Y211) and grain boundaries in the sample microstructure. In general, point, line and plane crystal defects and second phase inclusions increase $J_c$ by providing additional magnetic flux pinning sites. Grain boundaries, on the other hand, typically form a weak link between individual grains. This reduces $J_c$ and such boundaries should be avoided in order to optimize bulk behaviour.

A number of techniques have been developed to introduce defects in Y123 crystals, in addition to simple doping and the generation of oxygen vacancies by conventional solid state processes [10]. Columnar defects have been induced successfully in the micro structure by both ion beam irradiation and uranium fission [11,12] and line defects have been created by high-temperature deformation [13]. Y211 second-phase inclusions are incorporated in the Y123 matrix during peritectic solidification, essential to the melt process, which involves the interaction between Y211 particles and a Ba-Cu-O-based liquid to form the Y123 phase at temperatures between 1000 and 920°C in air. Fine Y211 inclusions can be engineered and dispersed in the Y123 matrix during this process to yield a high $J_c$ sample. Peritectic solidification processing has recently been adopted for the fabrication of YBCO wires [14,15], given its success in the growth of bulk materials.

Melt processed samples characteristically contain platelet boundaries in planes perpendicular to the *c*-axis of the lattice which form during the peritectic growth process [16,17]. Unreacted Ba-rich liquid has been reported to reside at these boundaries during processing which forms either an amorphous or crystalline phase on cooling. Individual platelet boundaries do not generally extent across the entire sample cross-section and the material can support a transport current via a percolation path through the specimen. Any misorientation of individual platelets, however, can limit the current carrying capability of the material significantly. $J_c$ is particularly sensitive to twist misalignment between grains [18,19], which should be avoided for transport current

*Published in: Applied Superconductivity (1996), vol. 4, iss. 10-11, pp. 507-517.*
*Status : Postprint (Author's version)*

applications.

To date bulk seeded melt processed YBCO samples have been fabricated with $J_c$ values of up to 80 000 A $cm^{-2}$ at 77 K in 1 T [20,21]. The magnitude and spatial variation of $J_c$ within these samples, however, are typically highly dependent on the microstructural and compositional characteristics of the specimen. In general, seeded melt processed samples exhibit greatest microstructural uniformity in the vicinity of the single crystal $SmBa_2Cu_3O_{7-\delta}$ seed placed on the sample surface prior to processing although this homogeneity decreases with distance from the seed position [9]. This fabrication technique minimizes the number of grain boundaries in the sample, although it may lead to an optimum individual pseudo-crystal size for specimens which exhibit uniformly high critical current densities [22].

The development of a high performance bulk YBCO conductor should be based on fabrication techniques which will introduce crystal defects and second-phase inclusions into the sample microstructure and on an effective joining process between large, individual grains of optimum size to yield high $J_c$ grain boundaries. The present study reports on the correlation between the growth morphology and grain boundary characteristics with critical current density in large grain melt processed YBCO. Such a correlation is not possible in any other material form.

## 2. EXPERIMENTAL

Large grain YBCO samples were fabricated by seeded and unseeded melt process techniques in order to investigate the properties of grain boundaries. A multi-grain sample was fabricated by a standard melt texture growth (MTG) [23] which involved heating a precursor pellet (diameter 29 mm and thickness 15 mm) of composition $Y_{1.6}Ba_{2.3}Cu_{3.3}O_{8.5\ \_\ \delta}$ (i.e. equivalent to a final phase composition of $YBa_2Cu_3O_{7-\delta} + 0.3Y_2BaCuO_5$) and 0.1 wt% platinum (Pt) metal to 1025°C in air in a tube furnace. The pellet was then cooled slowly (1°C $h^{-1}$) through the YBCO peritectic temperature (≈1000°C) to 920°C to yield a sample which consisted of a few large grains (typical dimensions of ≈5 mm) separated by well-defined grain boundaries, as illustrated schematically in Fig. 1.

***Fig. 1.*** *A schematic diagram illustrating the typical growth features in unseeded melt processed YBCO.*

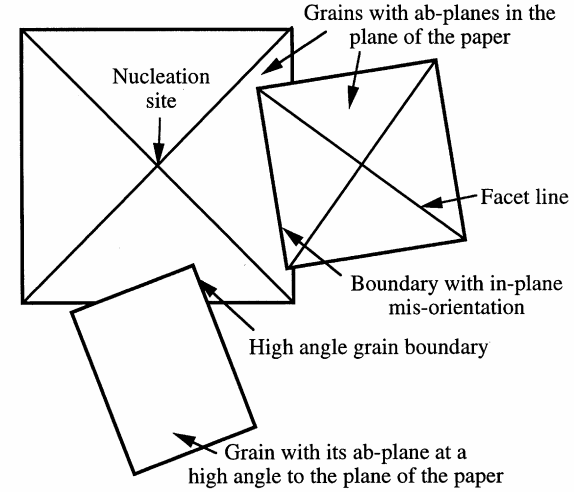


A second melt processed YBCO sample but consisting of a single large grain was fabricated by a controlled seeded peritectic solidification process [24] for studying the dependence of transport properties on microstructure within a grain. A precursor pellet of the same dimensions and composition as that used for MTG was melt processed under similar thermal conditions in a purpose-built thermal gradient furnace [25]. This contained four sets of independently controllable heating elements and a cold finger with a pointed tip, which is capable of generating a local cold point on the surface of the pellet during processing. A $SmBa_2Cu_3O_{7-\delta}$ seed, which has a similar crystallographic structure to but higher melting point than $YBa_2Cu_3O_{7-\delta}$, was placed on the surface of the pellet immediately under the point of the cold finger in order to generate a preferential nucleation site. The effect of this, with the heating elements set to produce increased temperature with distance from the seed, was to suppress the grain nucleation rate elsewhere on the surface and within the bulk of the pellet to facilitate controlled grain growth. Pellets which consist of only one grain can be prepared reproducibly by this technique.

*Published in: Applied Superconductivity (1996), vol. 4, iss. 10-11, pp. 507-517.*
*Status : Postprint (Author's version)*

The morphology and microstructure of both seeded and unseeded melt processed samples were examined using optical microscopy and scanning electron microscopy (SEM). Grain boundaries in the MTG sample which exhibited a significant variation in orientation between the adjacent grains were selected and isolated using a miniature wire saw. This process used a low cutting rate of about 10 $\mu mh^{-1}$ and a glycerol slurry containing 1200 mesh SiC particles in order to minimize damage to the boundaries during cutting. Typical as-cut sample sizes were 2 mm × 500 $\mu$m × 500 $\mu$m. Only samples where the boundary was clearly evident on both sides of the polished specimen were selected for measurement. Current and voltage leads were attached to these specimens at appropriate locations within the grains and across single grain boundaries. Ohmic contacts were fabricated by annealing Du Pont 6838 silver epoxy onto each sample at 420°C in flowing oxygen for 5 min. A four point AC (72 Hz) technique using EG&G low noise transformers and lock-in amplifiers was employed to measure the resistance and I-V characteristics of the specimens. This method avoids problems associated with thermal EMFs and enables sub-nanovolt resolution to be achieved. The voltages in the grains and across the well-defined grain boundary were measured *simultaneously* as a function of temperature for different applied fields, field angles with respect to the crystal and boundary axes and also as a function of current. I-V characteristics were measured using a Keithley 220 current source and a 182 nanovoltmeter. The external field was applied with a conventional electromagnet. Temperature control of better than 20 mK was achieved with the experimental arrangement used for these measurements.

Electron probe micro-analysis (EPMA) was used to determine the distribution of Sm inside the large single grain sample in view of the reported influence of Sm contamination on the transport properties of seeded melt processed YBCO. Specimens of dimensions 2 mm × 2 mm × 2 mm were subsequently extracted from positions distant from the seed using a wire cutter for studying the influence of microstructural inhomogeneity on transport properties.

In order to study further the connectivity of boundaries between grains of different relative crystallographic orientation, rectangular blocks of YBCO with selected orientations were cut from YBCO single grains and subsequently joined together. The experimental arrangement for the YBCO block joining process is illustrated schematically in Fig. 2. This involved stacking one YBCO block on top of another and loading the arrangement with a pressure of about 0.5 MPa to ensure a firm contact at the interface. The blocks were then heated in air to a temperature between 920 and 1000°C where residual unreacted liquid from the melt process, stored at the platelet boundaries, was released to the interfacial region. The composition of this liquid phase is determined by the $YBa_2Cu_3O_{7-\delta}$ liquidus in the phase diagram illustrated schematically in Fig. 3 and will vary over this temperature range. The stable co-existence of $YBa_2Cu_3O_{7-\delta}$ and the liquid under these conditions and the driving force provided by the surface free energy of the YBCO blocks, however, causes YBCO in the vicinity of the interface to dissolve into the liquid which re-precipitates on cooling to form a new, joined boundary. A scanning Hall-probe device was used to study the magnetic field screening properties of the joined blocks in order to characterize the integrity of the boundary. This involved cooling the specimen to 77 K, applying a magnetic field of up to 0.2 T and scanning a Hall probe of spacial resolution 0.25 mm across the sample surface. The resulting field map was compared with the physical structure of the joined grains.

***Fig. 2.*** *A schematic diagram illustrating the joining of YBCO grains using a semi-solid regrowth process.*

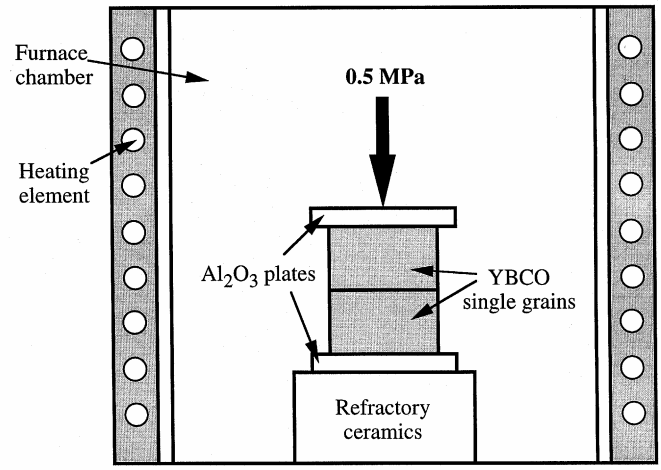

*Published in: Applied Superconductivity (1996), vol. 4, iss. 10-11, pp. 507-517.*
*Status : Postprint (Author's version)*

***Fig. 3.*** *A schematic diagram illustrating the segregation of liquid from platelet boundaries at high temperatures.*

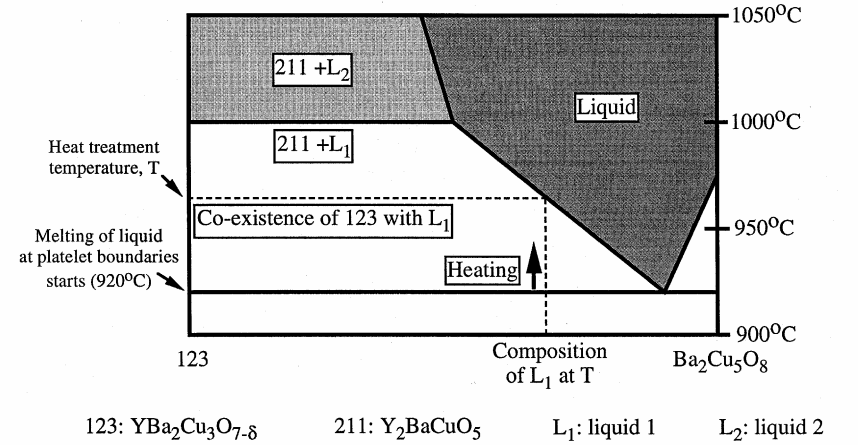


## 3. RESULTS AND DISCUSSION

The SEM micrograph in Fig. 4 shows the growth morphology at the surface of a large seeded YBCO grain in the vicinity of its nucleation site. The orientation of the *a-b* plane of the Y123 matrix was controlled by a seed and hence lies in the plane of the micrograph. A prominent feature on the surface of the grain is the presence of parallel lines which are oriented perpendicular to the macroscopic growth direction of the grain. It is well known that Y123 exhibits a pseudo-tetragonal crystal structure at the grain growth temperature and that preferred grain growth occurs along the lattice *a*- or *b*-axes. Hence it may be concluded that the lines in Fig. 4 are perpendicular to either the *a*- or *b*-axis of the lattice (and hence simultaneously parallel to the other).

Under higher magnification these lines were observed to be composed of layers of $YBa_2Cu_3O_{7-\delta}$ with parallel edges, as shown by the SEM micrography in Fig. 5. They correspond, therefore, to the *a*- or *b*-axis facet lines derived from the tetragonal symmetry in the *a-b* plane of Y123. The presence of continuous facet lines up to a distance of about 4 mm from the nucleation site suggests that uniform grain growth occurs in this region of the seeded melt processed YBCO sample. A homogeneous microstructure, associated with uniform grain growth, is observed in this region of the sample.

***Fig. 4.*** *A low magnification SEM micrograph showing the general growth morphology of the surface of a large melt processed YBCO grain. The presence of growth facets perpendicular to the macroscopic growth direction indicates that the grain was grown with a homogeneous planar growth front.*

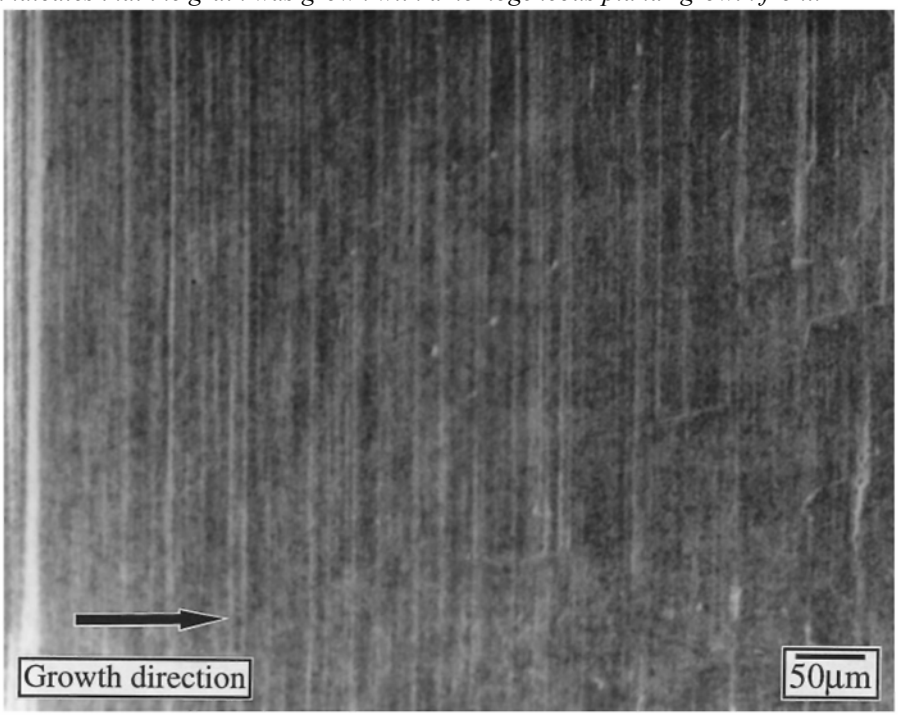

*Published in: Applied Superconductivity (1996), vol. 4, iss. 10-11, pp. 507-517.*
*Status : Postprint (Author's version)*

***Fig. 5.*** *A high magnification SEM micrograph showing the structure of growth facets.*


Microstructural inhomogeneity appears at positions more distant from the nucleation site, as illustrated by the SEM micrograph in Fig. 6 which was obtained from a position of about 6 mm from the seed. Apart from the identifiable Y123 phase edge in the micrograph, the $YBa_2Cu_3O_{7-\delta}$ layer at this location is fragmented and the continuous facet line is lost. Furthermore, the micrograph also shows the appearance of boundaries which divide the YBCO grain into sections, across which there may be a crystallographic mismatch. The density of such microstructural inhomogeneity increases with the distance from the nucleation site until the whole grain is composed of individual sections, or cells, of YBCO. It is clear that such microstructural inhomogeneity cannot develop from a uniform YBCO growth front. It is more likely that this microstructure signifies a change from a uniform to a near cellular growth morphology as the growth front advances through the Y211-liquid peritectic region. The occurrence of a non-uniform YBCO growth front has been observed in quenched pellets which contain partially grown YBCO grains and peritectic regions consisting of Y211 and solidified liquid. An example of such a morphology is shown in the SEM micrograph in Fig. 7, where a regular deviation from uniform planar growth is apparent.

The transition from a uniform to a non-uniform growth morphology may be understood by considering the Y123 peritectic solidification process. Solid Y211 particles dissolve into the liquid during the advancement of YBCO growth fronts to provide the Y cations required for the solidification of Y123 which subsequently diffuse through the liquid. Consequently, a homogeneous concentration distribution of Y in the liquid is critical to sustaining a uniform YBCO growth front. Local development of YBCO dendrites may occur, however, if the Y distribution in the liquid is not uniform. In view of the discrete nature of the Y211 particles, a change in their number density or volume proportion in the liquid may subsequently result in a local pile-up or deficiency of Y cations. This will, in turn, result in the development of local growth inhomogeneities [26,27].

A detailed analysis of the distribution of 211 inclusions in the 123 matrix from the nucleation site to a distance of 8 mm in a YBCO grain revealed that both the number density and volume proportion of Y211 inclusions increases gradually from the nucleation site, tending to a saturated value of about 30% at a distance of about 4 mm from the seed [28]. This corresponds to the region where the transition between uniform and non-uniform growth front morphology occurs. A change in the number density and proportion of Y211 particles in the liquid, or similarly the local non-uniform distribution of Y, may therefore account for the observed loss of microstructural homogeneity.

*Published in: Applied Superconductivity (1996), vol. 4, iss. 10-11, pp. 507-517.*
*Status : Postprint (Author's version)*

***Fig. 6.*** *A SEM micrograph showing the presence of growth inhomogeneity on the surface of a large YBCO grain at a location ≈4 mm from the nucleation site.*

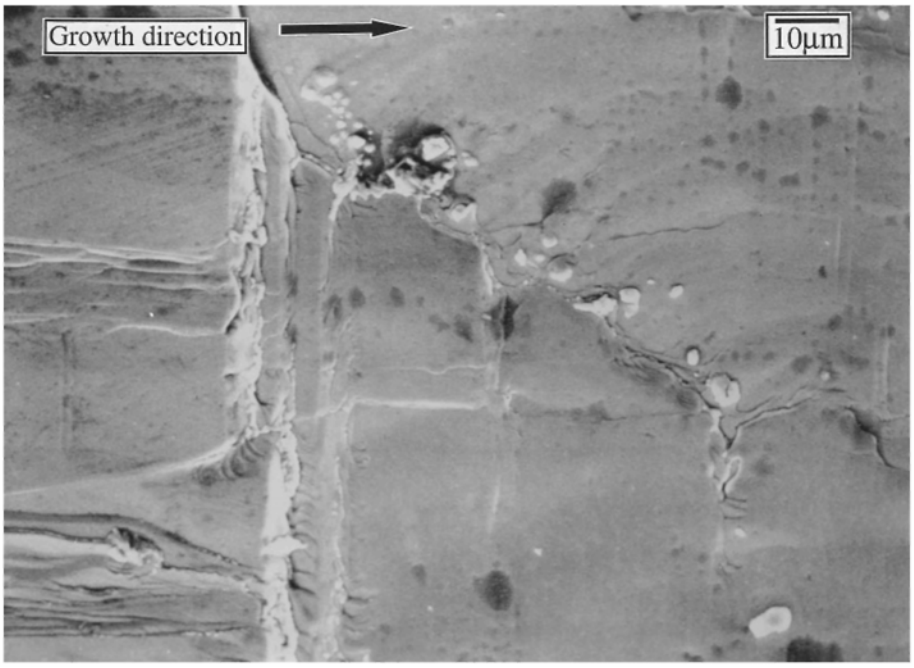


***Fig. 7.*** *A SEM micrograph showing the non-uniform growth front of a YBCO grain.*

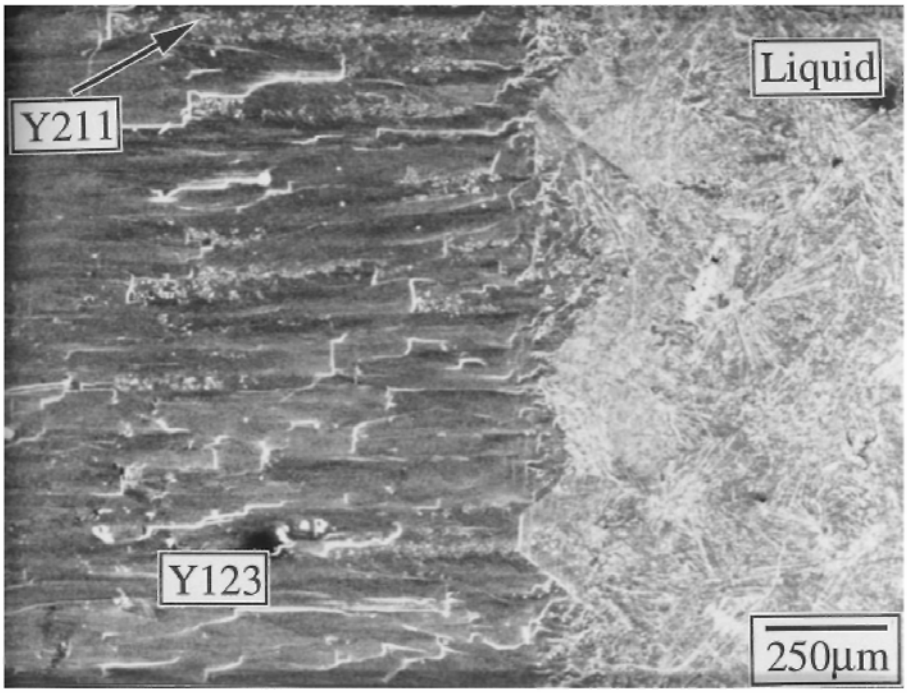


Figure 8 shows the positions in a large YBCO grain where specimens were obtained for the study of the influence of microstructural inhomogeneity on superconducting transport properties. Specimens were cut from a single layer ≈4mm beneath the surface of the large grain sample, rather than from the upper part of the specimen where the nucleation of the YBCO grain occurs, in order to minimize the effect of Sm contamination which would influence the transport properties (previous studies have revealed that Sm contamination is confined to a hemisphere of radius 3-4 mm from the centre of the seed [29]). The absence of Sm contamination was confirmed by the measured $T_c$s of the specimens, which were all at least 90 K (Sm contamination reduces $T_c$ significantly [30]). The average intragranular $J_c$ of each specimen at 1 T was extracted using the Bean model [31] from the width of the magnetic hysteresis loop measured by vibrating sample magnetometry. The variation of $J_c$ with

*Published in: Applied Superconductivity (1996), vol. 4, iss. 10-11, pp. 507-517.*
*Status : Postprint (Author's version)*

specimen position for temperatures between 5 and 77 K is shown in Fig. 8. It is clear from this figure that the $J_c$ of the YBCO sample decreases radially with distance from the centre of the grain over the entire superconducting temperature region. This variation in $J_c$ may be correlated with the development of microstructural inhomogeneity, given that there is no significant Sm contamination to influence the transport properties of the specimens.

Although the presence of growth inhomogeneities in seeded melt processed samples tends to lower $J_c$ such as regions of YBCO divided by local, occasional grain boundaries, the value of $J_c$ overall remains high in comparison with ceramic materials where a large number of grain boundaries coexist. This is due primarily to the low mismatch angles between grains in the former, compared with small grains in polycrystalline samples which join characteristically at high, random angles. High angle grain boundaries are also commonly observed in unseeded melt textured samples where typically more than one YBCO grain is grown in each pellet. The SEM micrograph in Fig. 9(a) shows the morphology of such a high angle grain boundary between unseeded melt processed YBCO grains. It can be seen that the surface of one of the grains is smooth and featureless whereas *a*- or *b*-axis facet lines are apparent on the surface of the other. It may be concluded, therefore, that the *a*-*b* planes of the two grains shown in this figure are twisted significantly with respect to each other to define a large misorientation and hence a poorly connected boundary. This boundary structure is illustrated further by the schematic diagram in Fig. 9(b).

***Fig. 8.*** *Radial variation of $J_c$ within a YBCO grain at positions free from Sm contamination by the seed.*

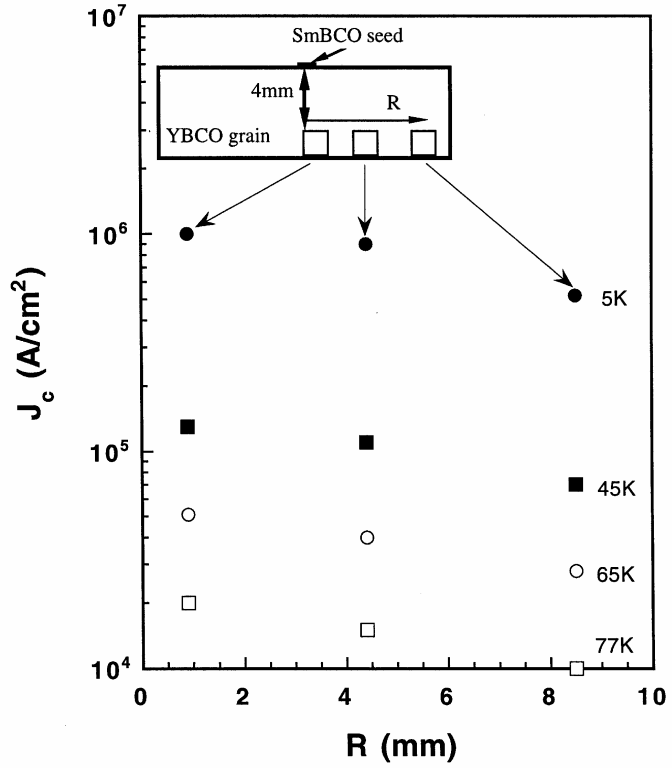

*Published in: Applied Superconductivity (1996), vol. 4, iss. 10-11, pp. 507-517.*
*Status : Postprint (Author's version)*

***Fig. 9.*** *(a) A SEM micrograph showing the morphology of a high angle boundary between two YBCO grains, (b) A schematic diagram illustrating the misorientation between the a-b planes of the YBCO grains to define a high angle boundary.*

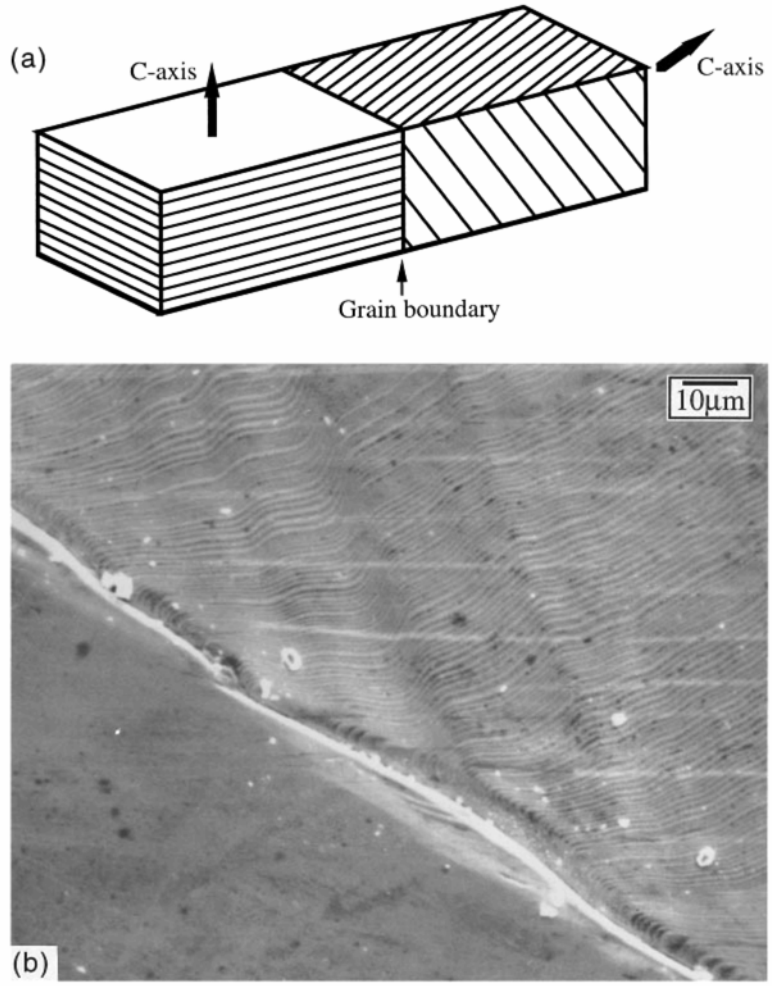


Figure 10 shows the variation of resistance with temperature within a YBCO grain (G) and across a high angle grain boundary (B), similar to the one in Fig. 9, for injection currents of 1 mA and 100 $\mu$A (i.e. corresponding to current densities of ≈0.05 and 0.005 A cm$^{-2}$, respectively). The resistive transition of the grain boundary is broadened considerably, even by a relatively small increase in injection current. The broad tail, which is distinct from the bulk superconducting transition, has the well-known form expected for thermally activated phase slippage (TAPS). The transition of one of the grains on the other hand is sharp and unaffected by the increased current. This is a clear indication that these measurements characterise the weakly linked grain boundary. The $J_c$ of this boundary was determined from I-V measurements which show a sharp onset of voltage at the critical current. This behaviour is characteristic of "clean" Josephson-like boundaries and is very different in form to the much more "rounded" I-V characteristics of the grains [32]. The $J_c$ for this boundary is less than 100 A cm$^{-2}$ at 77 K in zero applied field, which is more than two orders of magnitude lower than the measured intragranular $J_c$. It may be concluded, therefore, that the ability of melt textured YBCO to carry current is reduced significantly by the presence of high angle twist grain boundaries in the microstructure.

The connectivity of low angle grain boundaries differs markedly compared with their high angle counterparts, as illustrated by Fig. 11. This shows a Hall probe map of the surface of two YBCO grains joined along their *c*-axis (i.e. with effectively no mismatch angle) in an external magnetic field of 10 mT in a field screening arrangement [33]. The position of the grains and the boundary and the magnitude of the field normal to the sample surface are indicated in the diagram. The measurement was made by zero-field-cooling the sample to below $T_c$. A field was then applied when the temperature had stabilized at 77 K. Above the penetrated field, flux begins to enter the sample but is impeded by defects which act as pinning centres and a flux density gradient, or critical state [31], is established within the grains. This gradient is directly related to the pinning strength or critical current density of the material. Two possible scenarios prevail for a gain boundary or joint in the presence of an applied magnetic field. If the flux pinning force at the joint is weak and the critical current low, magnetic flux will penetrate

readily between the grains and they will behave like two separate specimens [33]. However, this is not observed from the magnetic field distribution in Fig. 11. On the contrary, the magnetic field is a minimum at the position of the boundary, which implies that superconductivity at the boundary is comparable with that inside the grains. Similar results were also observed when the external magnetic field was increased to 0.2 T. This suggests that artificial low angle joints between melt processed artefacts can be fabricated without a significant reduction in the current carrying ability of the joint relative to the grains. It may be concluded, therefore, that a low angle boundary does not necessarily impose a limitation to the transport properties of melt processed YBCO materials.

***Fig. 10.*** *A comparison of the resistance within a YBCO grain and across a high angle boundary between two YBCO grains.*

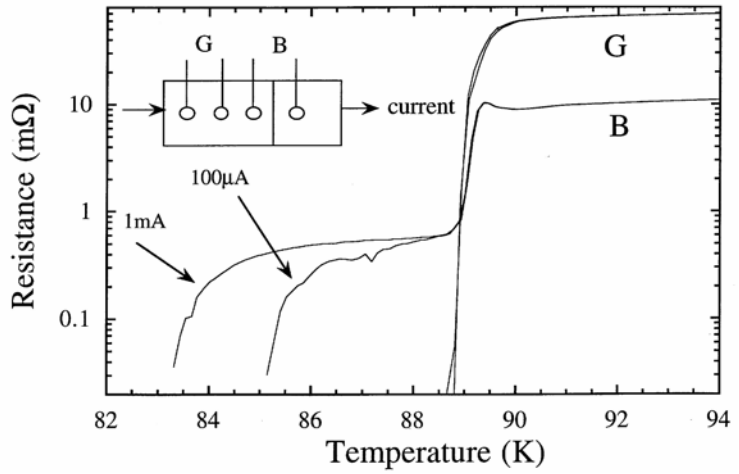


***Fig. 11.*** *The distribution of magnetic field on the surface of two joined YBCO grains in the presence of a 10 mT external magnetic field.*

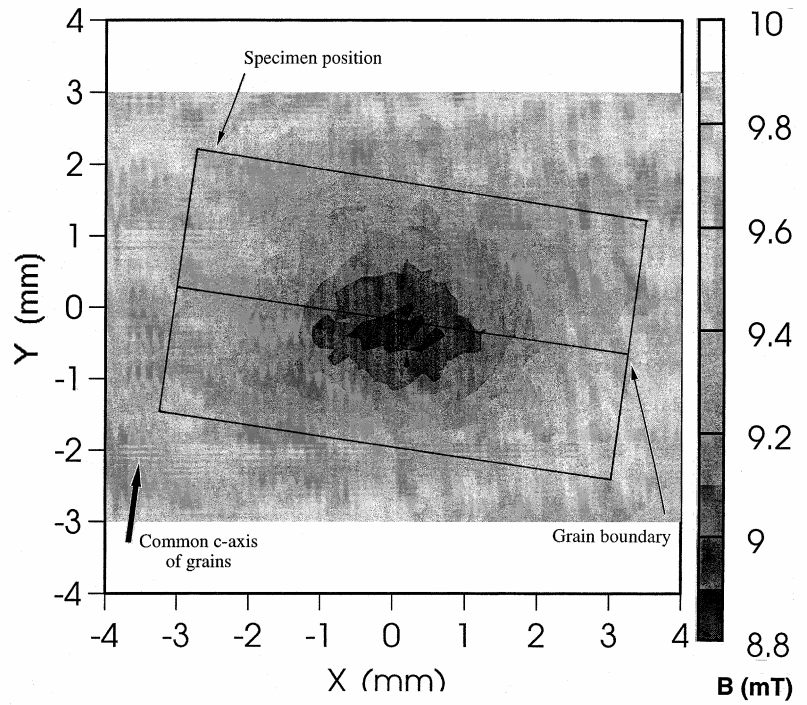


## 4. CONCLUSIONS

The transport properties within individual grains and across grain boundaries have been investigated and correlated with features in the micro structure of large grain melt processed samples fabricated by seeded and unseeded techniques. The presence of growth facets in the vicinity of the seed suggest that the YBCO grain initially grows uniformly up to a distance of about 4 mm from the nucleation site. The micro structure of the melt

processed YBCO sample is homogeneous in this region of growth. The facet growth lines disappear at greater distances from the seed; however, the micro structure becomes more cell-like and planar growth is lost due primarily to a variation in local yttrium concentration. A saturation in inclusion density and volume proportion of Y211 particles has been correlated with the appearance of the cell-like growth morphology which relates clearly to a variation in Y concentration. A decrease in critical current density with distance from the seed has been observed at temperatures between 5 and 77 K in samples which are not contaminated by Sm. This, again, correlates well with the development of micro structural inhomogeneity in the specimens.

High *c*-axis angle grain boundaries have been fabricated and isolated in unseeded melt processed YBCO samples. The resistance of such boundaries on transition to the superconducting state, which is generally broad, is observed to depend critically on the magnitude of the injection current. The intragranular resistance, however, is not influenced significantly by this variable. $J_c$ of the boundary was estimated to be less than 100 A $cm^{-2}$ at 77 K in zero applied field, which is more than two orders of magnitude lower than the intragranular $J_c$. The ability of melt processed YBCO to carry transport current is reduced significantly by the presence of high angle twist grain boundaries in the microstructure. Field screening measurements, on the other hand, suggest that low angle grain boundaries do not form weak links between grains in modest magnetic fields and hence do not present such a barrier to current flow.

## Acknowledgements

The authors gratefully acknowledge the support of the Croucher Foundation and International Energy Systems Ltd during this research. Ph. Vanderbemden is grateful to the F.N.R.S. for the provision of a research grant and to the Communauté Française de Belgique for a travel grant for this work.

## References

1. R. Tournier, E. Beaugnon, D. Bourgault, X. Chaud, P. Gautier-Picard, J. Noudem, A. Erraud, P. Tixador, M. Barrault, J. M. Barbut, O. Belmont, L. Porcar and J. Sanchez, *1st SCENET Workshop on Superconducting Materials for Power Applications,* Kassel, Germany, 10-12 April, (1997).

2. S. Jin, T. H. Tiefel, R. C. Sherwood, R. B. Van Dover, M. E. Davis, G. W. Kammlott and R. A. Fastnacht, *Phys. Rev. B* 37, 7850 (1988).

3. M. Murakami, M. Morita, K. Doi and M. Miyamoto, *Jap. J. Appl. Phys.* 28, 1189 (1989).

4. V. Selvamanickam and K. Salama, *Appl. Phys. Lett.* 57, (1990).

5. D. Shi, M. M. Fang, J. Akerjieze, M. Xu and J. G. Chen, *Appl. Phys. Lett.* 51, 2606 (1990).

6. P. McGinn, N. Zhu, W. Chen, S. Sengupta and T. Li, *Appl. Phys. Lett.* 57, 203 (1991).

7. L. Gao, R. L. Meng, Y. Y. Xue, P. H. Hoe and C. W. Chu, *Appl. Phys. Lett.* 58, 92 (1991).

8. L. Zhou, P. X. Zhang, P. Li, K. G. Wang, J. R. Wang and X. Z. Wu, *Supercond. Sci. Technol.* 3, 490 (1990).

9. W. Lo, D. A. Cardwell, C. D. Dewhurst and S. L. Dung, *J. Mater. Res.* 11, 786 (1996).

10. K. Salama and V. Salvamanickam, Melt processing and properties of Y-Ba-Cu-O, *Processing and Properties of High* $T_c$-*Superconductors, Vol. 1 Bulk Materials,* ed. S. Jin, World Scientific, Singapore, (1993), p. 155.

11. R. Weinstein, *World Congress on Superconductivity III,* Munich, Germany, ed. C. Burnham, Pergamon, Oxford, (1992), p. 1145.

12. R. Weinstein, R.-P. Sawh, Y. Ren and J. Liu, *Adv. Supercon. IX* 1, 539 (1997).

13. D. Rodgers, K. White, V. Selvamanickam, A. McGuire and K. Salama, *Supercond. Sci. Technol.* 5, 640 (1992).

14. Y. Nakamura, K. Furuya, T. Izumi and Y. Shiohara, *J. Mater. Res.* 9, 1350 (1994).

15. M. J. Cima, M. C. Flemings, A. M. Figuredo, M. Nakade, H. Ishii, H. D. Brody and J. S. Haggarty, *J. Appl. Phys.* 72, 179 (1992).

16. Y. Yan, D. A. Cardwell, A. M. Campbell and W. M. Stobbs, *J. Mater. Res.* 11, 2990 (1996).

17. W. Lo, D. A. Cardwell and J. C. L. Chow, *J. Mater. Res.* (in press), (1997).

18. D. Dimos, P. Chaudhari, J. Mannhart and F. K. LeGoues, *Phys. Rev. Lett.* 61, 219 (1988).

19. D. Dimos, P. Chaudhari and J. Mannhart, *Phys. Rev. B* 41, 4038 (1990).

20. I.-G. Chen, J. Liu, R. Weinstein and R. Shaw, *9th Int. Symp. on Superconductivity,* October, Sapporo, Japan, (1996).

21. R. Weinstein, J. Liu, Y. Ren, R.-P. Sawh, D. Parks, C. Foster and V. Obot, *10th Anniversary HTS Workshop on Physics,* March, Houston, TX, (1996).

22. R.-L. Meng, L. Gao, P. Gautierpicard, D. Ramirez, Y. Y. Sun and C. W. Chu, *Phys. C* 232, 337 (1994).

23. M. Murakami, *Supercond. Sci. Technol.* 5, 185 (1992).

24. W. Lo, D. A. Cardwell, C. D. Dewhurst, H.-T. Leung, J. C. L. Chow and Y. H. Shi, *J. Mater. Res.* (1997) (in press) .

25. D. A. Cardwell, W. Lo, H. D. E. Thorpe and A. Roberts, *J. Mater. Sci. Lett.* 14, 1444 (1995).

26. W. Lo, H.-T. Leung, D. A. Cardwell and J. C. L. Chow, *J. Am. Ceram. Soc.* 80, 813 (1997).

27. J. C. L. Chow, H.-T. Leung, W. Lo and D. A. Cardwell, *J. Mater. Sci.* (submitted), (1996).

28. D. A. Cardwell, W. Lo, H.-T. Leung and J. C. L. Chow, *Adv. Supercon. IX* 2, 725 (1997).

29. W. Lo, D. A. Cardwell and P. D. Hunneyball, *J. Mater Res.* (1997) (in press) .

30. C. D. Dewhurst, W. Lo and D. A. Cardwell, *IEEE Trans. Appl. Supercond.* 7, 1925 (1997).

31. C. P. Bean, *Rev. Mod. Phys.* 36, 31 (1964).

32. C. Sarma, G. Schindler, D. G. Haase, C. C. Koch, A. I. Kingon and A. Goyal, *Phys. C.* 244, 287 (1995).

33. X. H. Jiang, D. M. Astill, W. Lo, D. A. Cardwell, T. A. Coombs, A. M. Campbell and J. G. Larsen, *Phys. C* 249, 171 (1995).